Supramolecular Chemistry of $[\{M(CO)_3(\mu_3\text{-}OH)\}_4]$ (M = Mn or Re): A Modular Approach to Crystal Engineering of Superdiamondoid Networks†

Steven B. Copp, K. Travis Holman, Jeffrey O. S. Sangster, S. Subramanian and Michael J. Zaworotko*

Department of Chemistry, Saint Mary's University, Halifax, Nova Scotia, B3H 3C3, Canada

The compounds $[\{M(CO)_3(\mu_3\text{-}OH)\}_4]$ (M = Mn **1** or Re **2**), which are cubane-like molecules possessing T_d symmetry with four strong hydrogen-bond donor moieties rigidly directed towards the vertices of a tetrahedron, cocrystallized with 2 equivalents of a series of linear difunctional hydrogen-bond acceptor molecules or 'spacers' to afford 14 three-dimensional superdiamondoid networks with varying, but predictable, extents of interpenetration according to X-ray crystallography. The extent can be rationalized on the basis of the volume and length of the spacer molecule: benzene, toluene, *p*-xylene, *p*-fluorotoluene, naphthalene, 1-methylnaphthalene (all *via* π-hydrogen bonds), *N,N,N',N'*-tetramethylethane-1,2-diamine (tmen), 1,2-bis(diphenylphosphoryl)ethane (dppoe) and 1,4-diaminobenzene (dab) afford two-fold networks; 1,2-diaminoethane (en) and 2-chloropyrazine (cpyz) afford three-fold networks; 4,4'-bipyridyl (bipy) and 4,4'-bipiperidine (bipip) afford four-fold networks. The adducts **1**·2dppoe, **2**·2dab, **1**·2bipy, **2**·2bipy and **1**·2bipip crystallize with enough space in the crystal lattice to enclathrate one, four, two, two and two acetonitrile molecules per molecule of cubane, respectively. All fourteen networks crystallize in space groups that reflect at least some of the symmetry inherently present in **1** and **2**.

Exploitation of network hydrogen bonding in order to crystal engineer solids represents an area of considerable general and topical interest.[1] Whereas three-dimensional networks such as ice and KH_2PO_4 represent long and well known examples of tetrahedral self-assembly in the solid state,[2] the ability of appropriately tetrafunctionalized organic molecules with approximate S_4 symmetry to form superdiamondoid networks has only recently been subjected to study.[3] These networks are structurally analogous to diamond but the linkages are self-assembled hydrogen bonds rather than C–C bonds. In order to fill the space in the crystal lattice that is a consequence of large separations between the tetrahedral centres, the prototypal organic superdiamondoid compounds, adamantane-1,3,5,7-tetracarboxylic acid[3a] and 3,3-bis(carboxymethyl)glutaric acid ('methanetetraacetic acid'),[3b] undergo self-inclusion to exist as three- and five-fold independent networks, respectively. Although the networks interpenetrate there is no requirement for a measurable attraction between the networks other than the weakest of non-covalent interactions. The potential significance to inclusion chemistry was noted immediately and has subsequently been realized by work which demonstrates that such 'tectons' can be modified to afford inclusion of moderately sized guest molecules in the crystal lattice.[4] The term 'tecton' has been coined to define molecules which inherently have the requisite symmetry and functionality predictably to self-assemble.[4a] Unfortunately, there remain several drawbacks to the single component self-assembly approach: the very limited number of tetrafunctionalized molecules with the requisite symmetry and ability to self-assemble, their synthetic accessibility and the consequences upon the network superstructure of derivatizing them. We recently communicated[5] an alternative approach which has the potential to be far more versatile and general than single-component self-assembly: cocrystallization of a T_d molecule which contains four strong hydrogen-bond-donor groups but no strong hydrogen-bond-acceptor moieties with a linear difunctional hydrogen-bond-acceptor or 'spacer' molecule. Such a process, modular self-assembly of complementary molecules, will occur in a predictable fashion if the molecules do not have the functionality to self-assemble. In principle, modular self-assembly will permit substitution of a wide range of either T_d or linear 'spacer' molecules. It is important to distinguish between self-assembly of identical molecules and self-assembly of different but complementary molecules. The term *strict self-assembly*[6] would be appropriate to describe cocrystals formed by directed non-covalent interactions but does not necessarily exclude single-component self-assembly. Fig. 1 compares the single-component self-assembly and modular self-assembly approaches to construction of diamondoid networks. It should be noted that the approach shown in Fig. 1 is not the only multiple-component approach to crystal engineering of diamondoid solids. For example, two complementary S_4 moieties could cocrystallize.[7]

Our prototypal diamondoid compound, $[\{Mn(CO)_3(\mu_3\text{-}OH)\}_4]\cdot 2en$ **1**·2en (en = 1,2-diaminoethane) crystallizes in a cubic space group and consists of three interpenetrating superdiamondoid networks in which OH ··· en ··· HO hydrogen bonds serve as the geometric function of the C–C bonds in diamond itself. The network is superdiamondoid as a consequence of the T_d symmetry of **1**, a known and readily accessible molecule,[8] its four hydrogen-bond donor moieties which are rigidly directed towards the vertices of a tetrahedron, and the large separation between the tetrahedral centres. We have already demonstrated that the μ_3-OH moieties are strong hydrogen-bond donors since **1** is capable of forming 4:1 adducts with simple hydrogen-bond acceptors such as water and triphenylphosphine oxide.[9] Although **1** is a cubane-like molecule, in the context of this study it should simply be regarded as a rigid T_d tetrafunctional hydrogen-bond donor

---

† *Supplementary data available:* see Instructions for Authors, *J. Chem. Soc., Dalton Trans.*, 1995, Issue 1, pp. xxv–xxx.

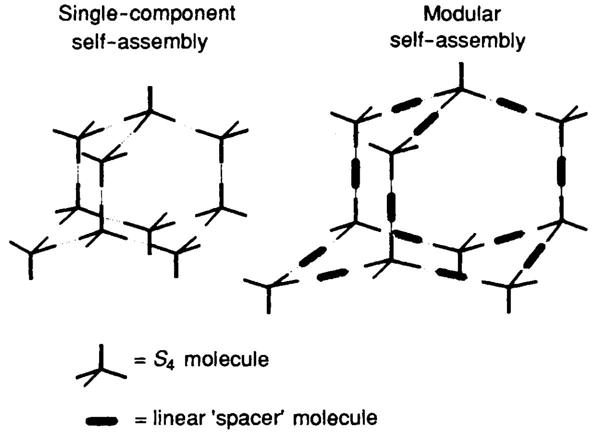

Fig. 1 Schematic representation of self-assembly and modular self-assembly in the context of superdiamondoid hydrogen-bonded networks

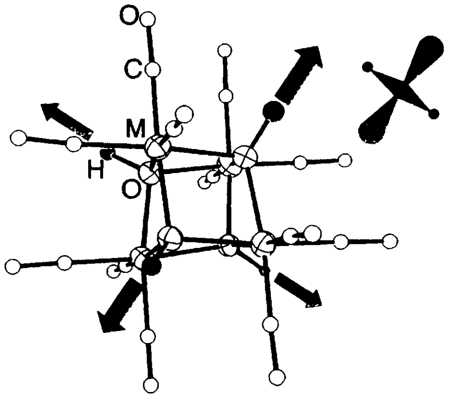

Fig. 2 Schematic of the tetrafunctional hydrogen-bond donors $[\{M(CO)_3(\mu_3\text{-}OH)\}_4]$ (M = Mn or Re) showing the tetrahedral orientation of the donor moieties

(Fig. 2). In this contribution we demonstrate that the modular self-assembly approach to construction of superdiamondoid networks is surprisingly facile and general and present full details of **1**·2en and thirteen other diamondoid networks formed from **1** or its rhenium analogue, **2**,[10] and twelve other 'spacer' molecules, including aromatic molecules which assemble superdiamondoid structures *via* bridge π-hydrogen bonding.

Results and Discussion

Compounds **1** and **2** readily cocrystallize with benzene, toluene, *p*-xylene, *p*-fluorotoluene, naphthalene, 1-methylnaphthalene, *N*,*N*,*N*′,*N*′-tetramethylethane-1,2-diamine (tmen), 1,2-bis(diphenylphosphoryl)ethane (dppoe), 1,4-diaminobenzene (dab), 1,2-diaminoethane (en), 2-chloropyrazine (cpyz), 4,4′-bipyridyl (bipy) or 4,4′-bipiperidine (bipip) to afford superdiamondoid networks with varying degrees of interpenetration, openness and distortion. All networks are based upon the ability of the second component or 'spacer' molecule to bridge adjacent molecules of **1** or **2** in a linear or approximately linear fashion. The spacer molecules are difunctional hydrogen-bond acceptors, meaning that the stoichiometry of each cocrystal is **1**·2spacer or **2**·2spacer. Crystallographic evidence suggests that the μ_3-OH moieties do not deprotonate even in the presence of the more basic hydrogen-bond acceptors since, as detailed in the Experimental section, OH hydrogen atoms were either located or refined. One might be surprised that arene molecules can serve as spacer molecules but this is indeed what occurs in the absence of more conventional hydrogen-bond acceptors. However, that O–H ··· arene π-hydrogen bonds can occur is precedented and a number of inter-[11–14] and intramolecular[15–17] attractions have been crystallographically characterized. The geometries of the spacer regions in ten of the superdiamondoid structures are depicted in Fig. 3 and reveal how each spacer serves the same crystal engineering function. The structures of the fourteen diamondoid solids are summarized individually and then discussed as a group.

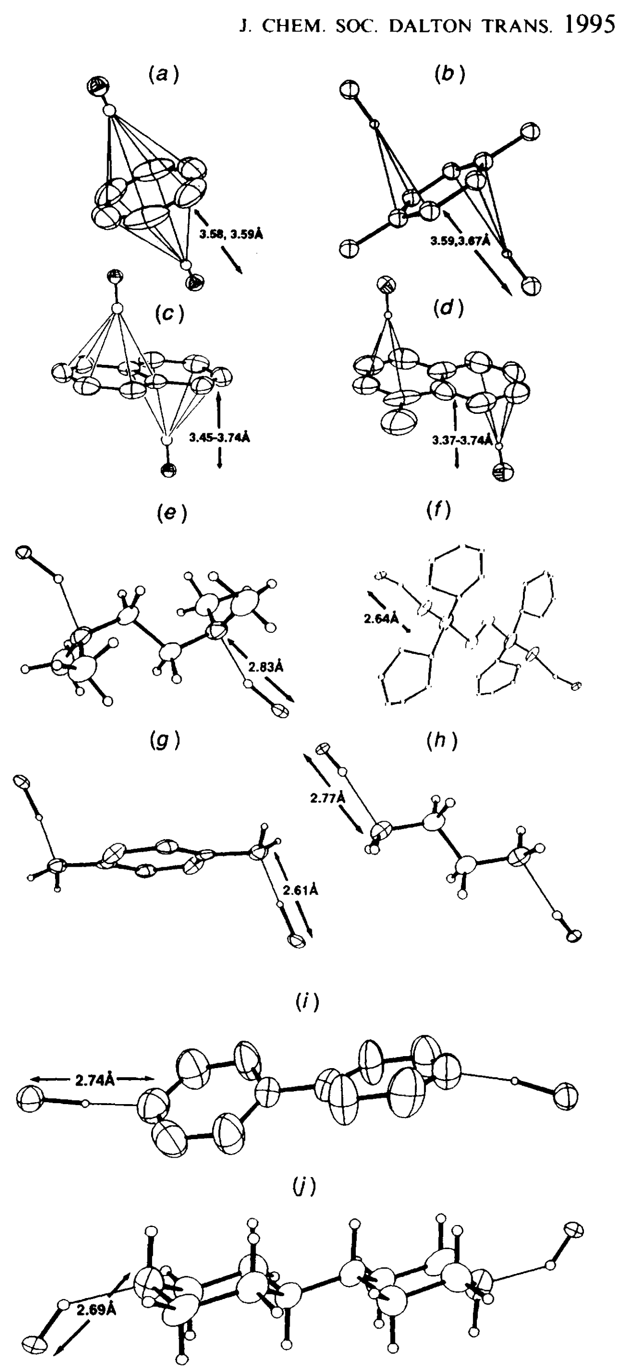

Fig. 3 Perspective views of the geometries around the spacer molecules in the bridging regions of the following cocrystals: (*a*) **1**·$2C_6H_6$, (*b*) **1**·$2C_6H_5Me$/**1**·$2C_6H_4Me_2$-1,4/**1**·$2MeC_6H_4F$-4, (*c*) **1**·$2C_{10}H_8$, (*d*) **1**·$2C_{10}H_7Me$-1, (*e*) **1**·2tmen, (*f*) **1**·2dppoe, (*g*) **2**·2dab, (*h*) **1**·2en, (*i*) **1**·2bipy and (*j*) **1**·2bipip. The O ··· C distances within 3.75 Å are indicated

1·$2C_6H_6$.—A two-fold (*i.e.* two interpenetrating but independent networks) undistorted superdiamondoid network is observed. An adamantoid portion of one of the networks and a simplified view of two interpenentrated adamantoid units are presented in Fig. 4. The diamondoid nature of the framework represents a manifestation of benzene acting as an acceptor to

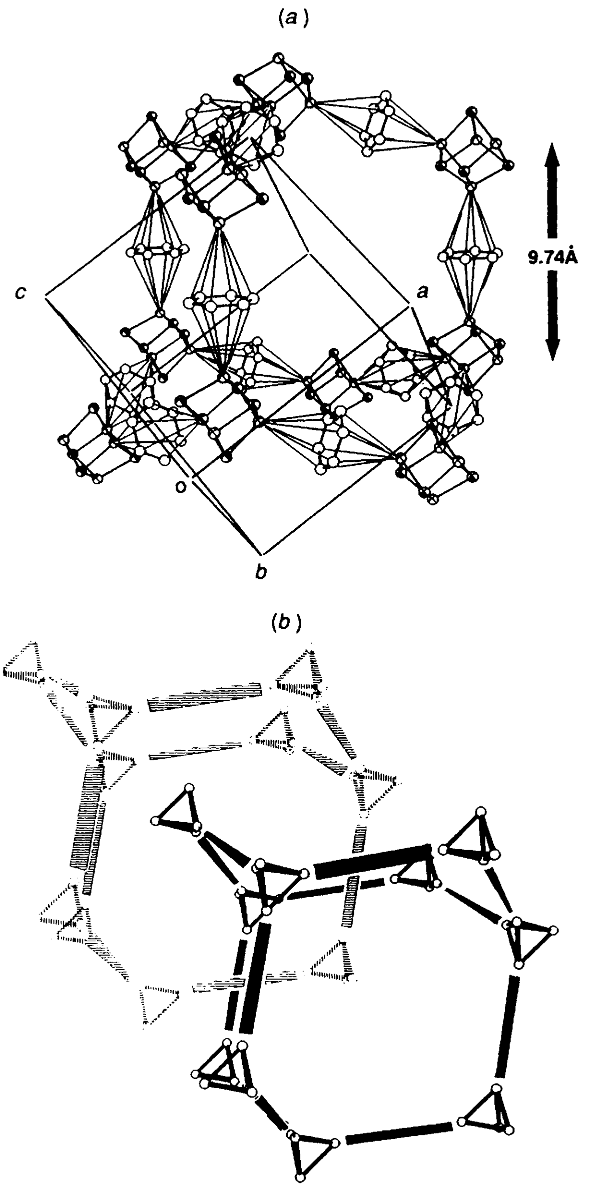

Fig. 4 (a) Perspective view of an adamantoid portion of one of the two superdiamondoid networks that exist in $\mathbf{1}\cdot2C_6H_6$. (b) A schematic of two interweaving adamantoid portions of the two-fold superdiamondoid network. Carbonyl ligands and hydrogen atoms have been omitted for clarity

π-hydrogen bonds at both of its faces. Therefore, even very weak non-covalent interactions[18] are capable of sustaining a superdiamondoid lattice framework. The bridge π-hydrogen-bonding mode has previously been proposed to explain the presence of benzene molecules in crystals of $[Mn_4(CO)_{12}\{\mu_3\text{-}F_x(OH)_{4-x}\}]\cdot2C_6H_6$ (in which the F and OH moieties are disordered) and $\mathbf{2}\cdot2C_6H_6$ but the consequences in terms of supramolecular architecture were not discussed.[11] The species $\mathbf{1}\cdot2C_6H_6$ deserves particular attention since benzene (point group D_{6h}) is the only one of the spacer molecules utilized herein that can sustain retention of the full T_d symmetry of **1**, and, even then, only if the bridging interaction retains three-fold symmetry. The observed interaction is indeed three-fold symmetrical and **1** lies around a crystallographic $\bar{4}3m$ or T_d position. Similarities in terms of space-group symmetry between $\mathbf{1}\cdot2C_6H_6$ and diamond itself would therefore be expected. Only six of two hundred and thirty space groups can hold $\bar{4}3m$ symmetry: $Fd\bar{3}m$ (adopted by diamond), $Pn\bar{3}m$ (adopted by $\mathbf{1}\cdot2C_6H_6$), $I\bar{4}3m$, $F\bar{4}3m$, $Fm\bar{3}m$ and $P\bar{4}3m$. The 'intercube' separation (*i.e.* the distance between the centres of adjacent molecules of **1** within the same network) is 9.74 Å, which predictably facilitates enough lattice space to self-include the second identical but independent network. Of the aforementioned six space groups, $Pn\bar{3}m$ is the only one that has two equivalent $\bar{4}3m$ sites. Therefore, for $\mathbf{1}\cdot2C_6H_6$, it is reasonable to assert that not only the crystal architecture but also the space group can be predicted with a reasonable degree of certainty.

Intermolecular OH ··· arene π-hydrogen bonds are presumably ubiquitous[11–14,19] but a recent study reveals only five examples of such interactions that are unambiguous according to X-ray crystallography,[20] none of which is of the bridging type encountered in this study. To our knowledge, $\mathbf{1}\cdot2C_6H_6$, $\mathbf{2}\cdot2C_6H_6$, $[Mn_4(CO)_{12}\{\mu_3\text{-}F_x(OH)_{4-x}\}]\cdot2C_6H_6$ and the subsequently described $\mathbf{1}\cdot2C_6H_5Me$, $\mathbf{1}\cdot2C_6H_4Me_2$-1,4, $\mathbf{1}\cdot2MeC_6H_4F$-4, $\mathbf{1}\cdot2C_{10}H_8$ and $\mathbf{1}\cdot2C_{10}H_7Me$-1 represent the only unambiguous X-ray crystallographic characterizations of arenes that bridge to both faces *via* O–H ··· arene ··· HO π-hydrogen bonds. Intermolecular O–H ··· arene π interactions have also been studied by spectroscopy[19] and rationalized through computational chemistry.[21] For water and benzene, the interaction appears to be symmetrical with O[H] ··· centroid distances of the order of 3.1–3.2 Å; N–H ··· arene[18,22] and C–H ··· arene[23–26] interactions with similar intermolecular contacts have also been recently observed. In $\mathbf{1}\cdot2C_6H_6$, in order to be classified as a π-hydrogen bond one would expect O[H] ··· C contacts to be within 3.75 Å,[27] and in the present study only O[H] ··· C distances less than this limit are reported. There are two O[H] ··· C contacts, 3.582(9) and 3.591(8) Å, because there is a slight chair distortion of the benzene. One would also expect the O–H infrared stretch to be shifted to lower wavenumber and broadened. It lies at 3572 cm^{-1} compared to 3633 cm^{-1} for unsolvated **1**.[28] The geometry of the bridging region is illustrated in Fig. 3(*a*).

$\mathbf{1}\cdot2C_6H_5Me$.—A two-fold tetragonally distorted superdiamondoid network is observed. Molecules of **1** lie around crystallographic $\bar{4}2m$ positions and the methyl groups of the toluene molecules are disordered. However, the disorder does not influence the interpretation or accuracy of the structure since the ring carbon atoms are unaffected. The architecture is similar to that of $\mathbf{1}\cdot2C_6H_6$ but the OH moieties are laterally slipped with respect to the C_6 ring. The interaction between the μ_3-OH ligands and the toluene molecules is therefore unsymmetrical [Fig. 3(*b*)], the diamondoid architecture is distorted, and the lattice symmetry is reduced from cubic to tetragonal. The O[H] ··· C(toluene) distances are 3.592(6) and 3.667(6) Å, close to the geometry and distances seen for a recently characterized unsymmetrical OH ··· arene intramolecular π-hydrogen bond between a silanol and a phenyl group {[O]H ··· C distances were 2.37(6), 2.65(6) and 2.61(6) Å}.[17] The intercube separation is 10.10 Å.

$\mathbf{1}\cdot2C_6H_4Me_2$-1,4 *and* $\mathbf{1}\cdot2MeC_6H_4F$-4.—The crystal structures are essentially isostructural to that of $\mathbf{1}\cdot2C_6H_5Me$ (including disorder of *p*-fluorotoluene) with enhanced tetragonal distortions, presumably to accommodate the larger volume requirements of *p*-xylene and *p*-fluorotoluene *vs.* toluene. The intercube separations are 10.35 and 10.13 Å, respectively. The O[H] ··· C(arene) distances are relatively long [3.651(6) and 3.750(5) Å for $\mathbf{1}\cdot2C_6H_4Me_2$-1,4; 3.585(11) and 3.679(11) Å for $\mathbf{1}\cdot2MeC_6H_4F$-4]. The fluorine atom of *p*-fluorotoluene does not act as a hydrogen bond acceptor for the μ_3-OH moieties even though C–H ··· F interactions have recently been shown to be controlling factors in crystal structures.[29] An adamantoid portion of one of the independent networks in $\mathbf{1}\cdot2MeC_6H_4F$-4 is illustrated in Fig. 5 and is similar to that of $\mathbf{1}\cdot2C_6H_5Me$ and $\mathbf{1}\cdot2C_6H_4Me_2$-1,4.

$\mathbf{1}\cdot2C_{10}H_8$.—Once again, the OH ··· arene interaction is

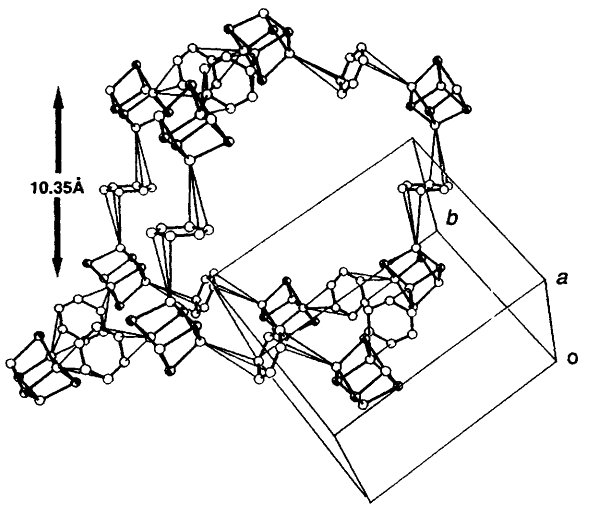

Fig. 5 Perspective view of an adamantoid portion of one of the two superdiamondoid networks that exist in **1**•2$C_6H_4Me_2$-1,4. Carbonyl ligands, methyl groups and hydrogen atoms have been omitted for clarity

laterally slipped but now it is directed towards two different C_6 arene rings. Furthermore, the naphthalene molecules are slightly twisted, resulting in molecules of **1** possessing $\bar{4}$ rather than $\bar{4}2m$ site symmetry. The O[H] ··· C(naphthalene) distances vary between 3.449(7) and 3.743(7) Å and the intercube separation is 10.40 Å. An ORTEP[30] view of the bridging region is illustrated in Fig. 3(*c*).

1•2$C_{10}H_7Me$-1.—One would expect the symmetry of the network to be reduced even further by the presence of the methyl group, perhaps to the extent of generating bulk polarity. The superdiamondoid network remains two-fold but one half of the 1-methylnapthalene molecules in each unit cell are disordered around crystallographic inversion centres, thereby precluding bulk polarity. The network possesses much lower crystallographic symmetry than that of the other arene cocrystals and adopts a hexagonal space group. The T_d symmetry of **1** is reduced to just three-fold symmetry in six of the twenty-four molecules in the unit cell and the remainder have no crystallographic symmetry. The O[H] ··· C($C_{10}H_7Me$) distances vary upward from 3.368(9) Å with intercube separations ranging from 10.26 to 10.53 Å. The bridging region of the ordered 1-methylnaphthalene is illustrated in Fig. 3(*d*).

1•2tmen.—A two-fold tetragonally elongated superdiamondoid structure occurs. An adamantoid portion of one network is illustrated in Fig. 6. Molecules of **1** lie around crystallographic two-fold axes. The two independent O[H] ··· N hydrogen-bond distances, 2.835(6) and 2.828(6) Å, are statistically identical and within expected ranges.[31] The space-group symmetry reveals that the structure can be described as a series of cross-linked helices similar to that seen for the disodium and dipotassium salts of adamantane-1,3,5,7-tetracarboxylic acid.[4c] The intercube separation is 11.35 Å. The geometry in the bridging region is illustrated in Fig. 3(*e*). It reveals how the tmen spacer molecule orients itself to bridge μ_3-OH moieties on adjacent molecules of **1**.

1•2dppoe.—The structure consists of two tetragonally distorted superdiamondoid networks formed from strong OH ··· O=P hydrogen bonds. Molecules of **1** lie 13.53 Å apart around crystallographic $\bar{4}$ positions so all four OH ··· $OPPh_2CH_2CH_2PPh_2O$ interactions are identical. The O[H] ··· O distances of 2.639(8) Å compare with the 2.563(8) Å observed in **1**•4$OPPh_3$.[9] One disordered molecule of acetonitrile is present within the lattice and the dppoe molecules are disordered around crystallographic inversion centres such that there are two orientations. One orientation and how it bridges the μ_3-OH moieties on adjacent molecules of **1** is illustrated in Fig. 3(*f*).

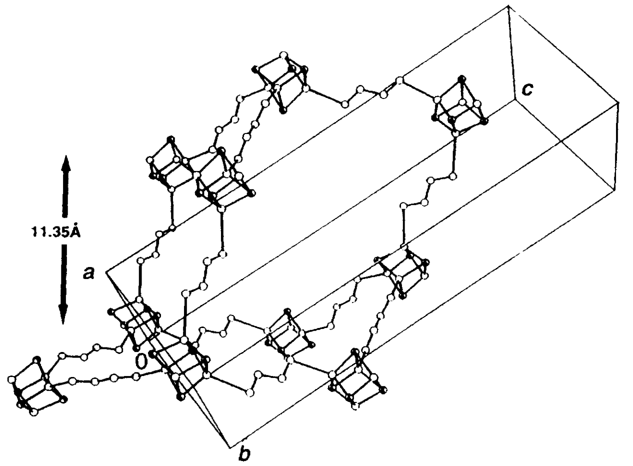

Fig. 6 Perspective view of an adamantoid portion of one of the two superdiamondoid networks that exist in **1**•2tmen. Carbonyl ligands, methyl groups and hydrogen atoms have been omitted for clarity

2•2dab.—Molecules of compound **2** lie 11.79 Å apart around crystallographic $\bar{4}$ positions whereas the bridging dab molecules lie around inversion centres. The tertiary structure consists of two independent diamondoid networks which are tetragonally contracted. The O[H] ··· N separations of only 2.608(18) Å are indicative of strong hydrogen bonds and the intramolecular distances within **2** are almost identical to those of **1**. An interesting feature of the structure concerns the observation that enough lattice space exists to accommodate four acetonitrile molecules per molecule of **2**, *i.e.* dab is too small to sustain a three-fold network and too large to sustain a close-packed two-fold network. Fig. 7 presents a view of the complete structure looking at the *ab* plane. The microchannels containing the acetonitrile molecules are parallel to the *c* axis. The geometry of the bridging region is presented in Fig. 3(*g*).

1•2en.—This species crystallizes in a cubic space group, $I\bar{4}3d$. Three independent networks interweave one another. Molecules of **1** lie around crystallographic $\bar{4}$ positions whereas en molecules lie around two-fold axes. The molecules of **1** are 11.59 Å apart, which compares with the 11.35 Å seen for the tmen analogue. The O[H] ··· N separations of 2.774(8) Å are consistent with what would be expected for N–H ··· O hydrogen bonds. The geometry of the bridging region is illustrated in Fig. 3(*h*).

1•2cpyz.—The structure of species **1**•2cpyz can be regarded as being isostructural with **1**•2en having a slightly larger cell volume (6.2%) and intercube separations (11.82 Å). This is perhaps unsurprising given the similarities between the geometries of the two spacer molecules in the critical bridging region. 2-Chloropyrazine was chosen because it does not inherently contain a centre of inversion or a two-fold axis and the resulting network could reasonably have been expected to be polar. Unresolvable crystallographic disorder generates two-fold symmetry but no crystallographic centre of inversion. An adamantoid portion of one of the networks is illustrated in Fig. 8. The slightly longer N ··· N separation in **1**•2en *vs.* **1**•2cpyz is compensated for by longer hydrogen-bond lengths in the latter, which are extremely long {O[H] ··· N 3.218(15) Å}. The long hydrogen-bond lengths might reasonably be a manifestation of the weak basicity of cpyz compared to en and, indeed, all the other spacers except for the arenes.

1•2bipy.—4,4′-Bipyridine represents a much longer spacer molecule than those detailed above. This is manifested in a

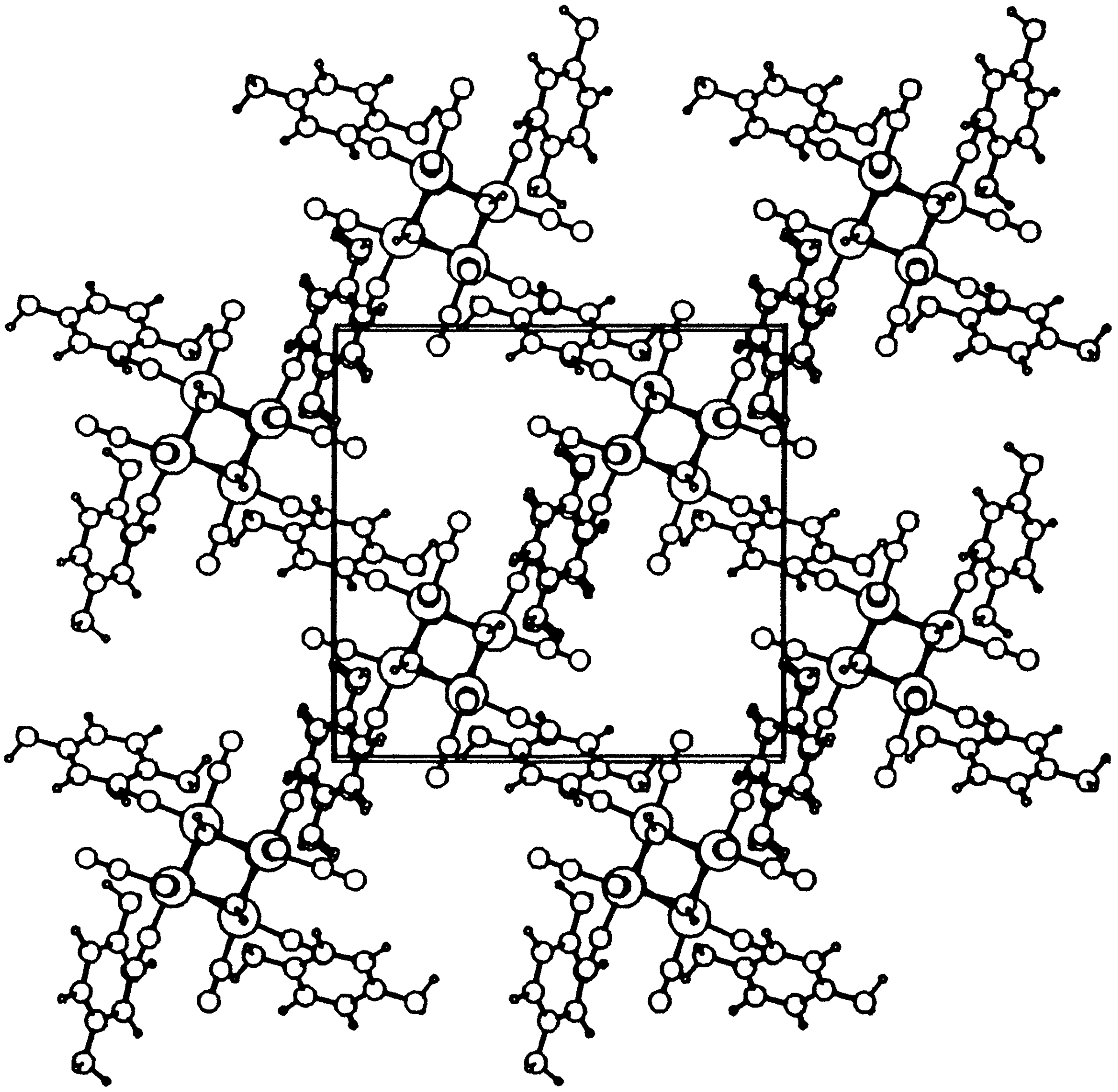

Fig. 7 Overhead view of the *ab* plane in **2**·2dab. The solvent molecules, omitted for clarity, lie in the channels formed parallel to the crystallographic *c* axis because the interweaved diamondoid networks cannot occupy all the space in the crystal

longer intercube separation, 15.22 Å. Once again compound **1** retains crystallographic $\bar{4}$ symmetry, meaning all four O[H] · · · N separations are identical [2.744(9) Å], and the bipy molecules lie around two-fold axes. The tertiary structure consists of four tetragonally elongated diamondoid networks arranged around a four-fold crystallographic axis (Fig. 9). This axis, which is parallel to the *c* axis, represents a microchannel running throughout the length of the crystal. The microchannel is large enough to contain two sites which are occupied by acetonitrile molecules. The latter appear to be dynamically disordered since the ^{1}H NMR spectrum of a solid sample obtained without magic angle spinning displays two singlets at δ 4.39 and 3.53. A view of the bridging region is illustrated in Fig. 3(*i*).

2·2bipy.—The crystal structure of this species is isomorphous with that of **1**·2bipy, including the inclusion of two acetonitrile solvent molecules, and there is virtually no change in any of the important parameters. For example, the cell volume increases by only 0.1% and the intercube separation goes from 15.22 to 15.24 Å. This appears to be the case because the slightly larger volume of **2** *vs.* **1** is compensated for by shorter hydrogen bonds, O[H] · · · N being only 2.51(4) Å.

1·2bipip.—The structure is closely related to those of **1**·2bipy and **2**·2bipy with four tetragonally elongated interweaved networks arranged around crystallographic four-fold axes and two independent acetonitrile molecules per molecule of **1** lying disordered on these axes, which are parallel to the *c* axis. The intercube separation, 15.35 Å, is slightly longer than those seen for the bipy-bridged networks and the O[H] · · · N separation is 2.690(7) Å. A representative view of an adamantoid portion of one of the independent networks is in Fig. 10 and the bridging region is illustrated in Fig. 3(*j*).

Comparison of 'Cube' Geometries.—The geometries of compounds **1** and **2** appear to be unaffected by their environment. Table 1 summarizes their important geometric features and reveals that the Mn–CO and Mn–O distances are within expected ranges.[32] The larger radius of Re *vs.* Mn manifests itself with slightly longer Re–CO distances and significantly longer Re–O distances.

Comparison of Crystal Architectures.—Table 2 summarizes the salient features of the fourteen new cocrystals. It should be apparent that a diverse range of superdiamondoid networks is

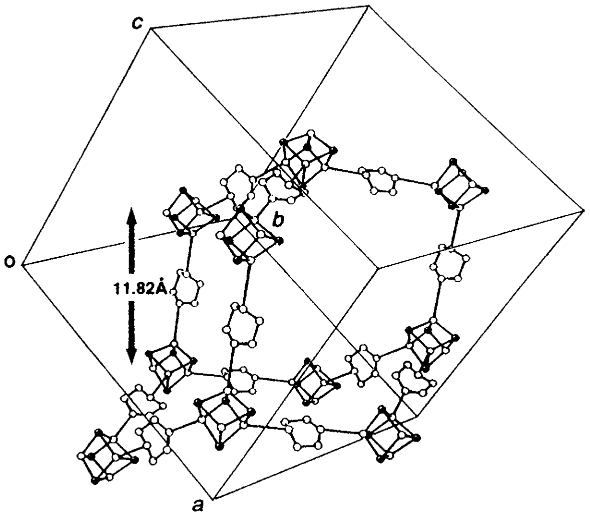

Fig. 8 Perspective view of an adamantoid portion of one of the three superdiamondoid networks that exist in **1**·2cpyz. Carbonyl ligands, methyl groups and hydrogen atoms have been omitted for clarity. The 2cpyz do not appear planar because of unresolvable crystallographic disorder

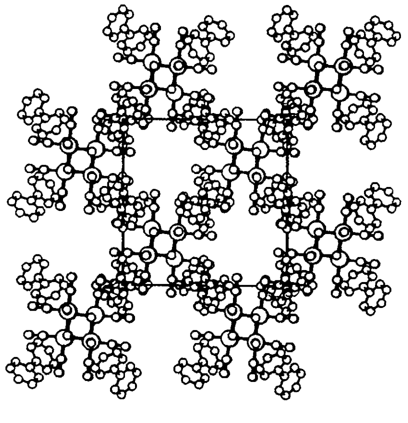

Fig. 9 Overhead view of the *ab* plane in species **1**·2bipy. Disordered MeCN solvent molecules, omitted for clarity, lie in channels around crystallographic four-fold axes parallel to the crystallographic *c* axis

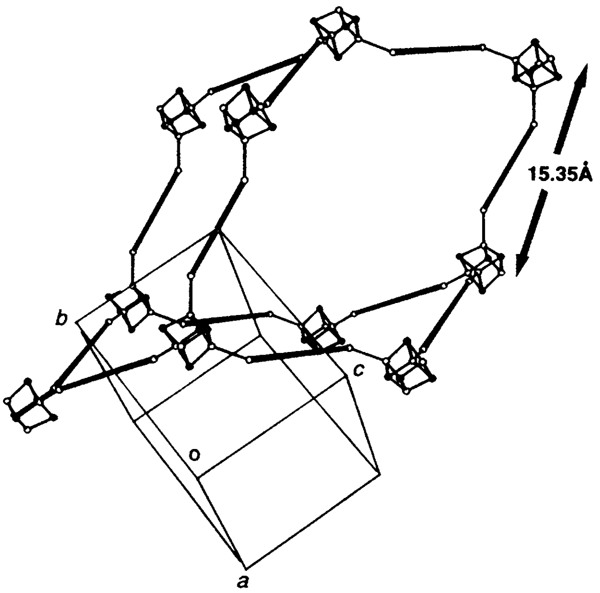

Fig. 10 Perspective view of an adamantoid portion of one of the four superdiamondoid networks that exist in **1**·2bipip. Carbonyl ligands and hydrogen atoms have been omitted and the bipip ligands are represented by solid lines for clarity

readily accessible *via* modular self-assembly of T_d molecules **1** or **2** and a variety of difunctional hydrogen-bond acceptor spacer molecules. It is remarkable that all but two of the fourteen crystal structures reported herein retain the S_4 axis of **1** and **2** in a crystallographic sense. Indeed, the crystal structures of the cocrystals described are predictable and logical given the geometric nature of **1** and **2** and the spacer molecules. Specifically, because the hydrogen-bond donor (*i.e.* μ_3-OH) and acceptor (*i.e.* basic nitrogen or oxygen atom, arene ring) moieties form relatively strong hydrogen bonds, are geometrically constrained and limited in number, the observed structures are the only ones that can utilize all the available good proton donors and the acceptors even if the latter are weak. The diamondoid networks therefore follow the simple rules that have been empirically derived for crystal packing of organic molecules.[1f] Whereas the spacer molecules are chemically diverse, they all have one key feature in common: a capability to act as a difunctional hydrogen-bond acceptor in which the vectors of the acceptor moieties are antiparallel. Spacers can therefore be either linear or zigzag and chemically different pairs of spacers such as en/cpyz and dab/dppoe afford essentially identical networks because their geometric features, specifically how the lone pairs are disposed, are so similar. The orientation of the hydrogen-bond-acceptor moieties within the spacer molecules is a necessary prerequisite for formation of the diamondoid architecture. For example, angular difunctional spacer molecules also cocrystallize with and exploit the T_d symmetry of **1** and **2**, however, two-dimensional 'chicken-wire' or carpet-like structures are obtained.[33] The limited number of acceptor moieties on the spacer molecules means that, except for en, there is no possibility for secondary or competing networking since there are no other competing proton donors or acceptors present. As might be expected, the volume of the spacer molecule is also relevant. This is best illustrated by **1**·2en and **1**·2tmen. Although the bridge geometries and therefore the intercube separations are similar, the degree of interpenetration decreases as the size of the ancillary groups increases.

There are several aspects of this study which bear broader relevance.

Design of diamondoid networks. In addition to the non-covalent examples of diamondoid networks mentioned in the Introduction there are a number of compounds which are known to consist of interpenetrating covalent diamondoid networks. The most notable of these are perhaps $Cd(CN)_2$,[34] polychalcogenides[35] such as $[Pd(Se_4)_2]^{2-}$ and $[Pd(Se_6)_2]^{2-}$, $Cd(SPh)_2$[36] and cationic Cu^I-based frameworks.[37] The first two systems are two-fold and $Cd(CN)_2$ exhibits a diverse range of structures depending upon the crystallization conditions, including the ability to form a one-fold network with enclathrated guests such as CCl_4,[38] $CHCl_3$[34] and water–cyclohexanol.[39] It is therefore not a prerequisite that the tetrahedral component has to utilize directed non-covalent interactions. Design criteria will hold for either non-covalent networks or for their covalent analogues. It should be noted that a recent study considered the potential for generating hard materials based upon interpenetrating covalent diamondoid networks.[40] The results reported herein can therefore be expected to be relevant in the context of the design and crystal engineering of both covalent and non-covalent networks, the key observation being that the modular approach is inherently facile and versatile, *i.e. any* tetrahedral component can in principle be exploited with a complementary spacer molecule. Furthermore, judicious choice of these modular components leads to, at least in some cases, a predictable crystal structure or

Table 1 Superdiamondoid networks based upon $[\{M(CO)_3(\mu_3\text{-}OH)\}_4]$ (M = Mn or Re) and difunctional spacer molecules

M	Spacer	Intercube distance/Å	Crystal system	Site symmetry	*n*-Fold	Solvent molecules	Centrosymmetric
Mn	C_6H_6	9.74	Cubic	$\bar{4}3m$	2		Yes
Mn[a]	C_6H_6	9.77	Cubic	$\bar{4}3m$	2		Yes
Re[b]	C_6H_6	9.82	Cubic	$\bar{4}3m$	2		Yes
Mn	C_6H_5Me	10.10	Tetragonal	$\bar{4}2m$	2		Yes
Mn	C_6H_4Me-1,4	10.35	Tetragonal	$\bar{4}2m$	2		Yes
Mn	MeC_6H_4F-4	10.13	Tetragonal	$\bar{4}2m$	2		Yes
Mn	$C_{10}H_8$	10.40	Tetragonal	$\bar{4}$	2		Yes
Mn	$C_{10}H_7Me$-1	10.26–10.53	Hexagonal	3, 1	2		Yes
Mn	tmen	11.35	Tetragonal	2	2		No
Mn	dppoe	13.53	Tetragonal	$\bar{4}$	2	MeCN	Yes
Re	dab	11.79	Tetragonal	$\bar{4}$	2	4MeCN	Yes
Mn	en	11.59	Cubic	$\bar{4}$	3		No
Mn	cpyz	11.82	Cubic	$\bar{4}$	3		No
Mn	bipy	15.22	Tetragonal	$\bar{4}$	4	2MeCN	Yes
Re	bipy	15.24	Tetragonal	$\bar{4}$	4	2MeCN	Yes
Mn	bipy	15.35	Tetragonal	$\bar{4}$	4	2MeCN	Yes

[a] A mixture of $[Mn_4(CO)_{12}F_x(OH)_{4-x}]$, see ref. 11(*a*). [b] See ref. 11(*b*).

Table 2 Comparison of geometries of compounds **1** and **2**

Adduct	M–C/Å	C=O/Å	M–O/Å	M–O–M/°	O–M–O/°
1·2C_6H_6	1.815(4)	1.129(7)	2.052(3)	102.37(18)	76.07(14)
1·2C_6H_5Me	1.814(1)	1.134(0)	2.052(1)	102.17(5)	76.31(3)
1·2$C_6H_4Me_2$-1,4	1.800	1.144(1)	2.058(4)	102.13(12)	76.36(8)
1·2MeC_6H_4F-4	1.809(7)	1.146(2)	2.048(3)	102.58(6)	75.77(5)
1·2$C_{10}H_8$	1.803(10)	1.148(5)	2.058(1)	102.13(9)	76.38(6)
1·2$C_{10}H_7Me$-1	1.791(13)	1.150(7)	2.055(9)	102.21(42)	76.26(25)
1·2tmen	1.798(9)	1.138(4)	2.042(13)	101.68(88)	76.94(60)
1·2dppoe	1.767(24)	1.165(20)	2.036(7)	101.74(20)	76.87(12)
2·2dab	1.862(54)	1.18(5)	2.184(3)	103.3(14)	75.0(9)
1·2en	1.784(9)	1.153(7)	2.033(9)	101.95(20)	76.60(13)
1·2cpyz	1.782(11)	1.163(9)	2.048(5)	101.79(111)	76.79(71)
1·2bipy	1.782(8)	1.158(9)	2.036(6)	101.98(41)	76.57(25)
2·2bipy	1.84(9)	1.21(3)	2.19(4)	102.6(4)	75.7(3)
1·2bipip	1.788(8)	1.152(3)	2.039(6)	101.39(80)	77.29(54)

even space group (as is the case for **1**·2C_6H_6). In the context of non-covalent networks it should be noted that a recent study by Ermer focused upon the complementary nature of hydroxy and amino groups. Their propensity to form 1 : 1 complexes can realize superdiamondoid architectures if appropriate dialcohols and diamines are cocrystallized.[41]

Inclusion chemistry. Five of the fourteen new structures described herein contain acetonitrile molecules that reside in microchannels running parallel to the crystallographic *c* axis in tetragonal space groups. Microchannels are a feature often associated with zeolites and related inorganic solids.[42] Zeolitic channels, although capable of including hydrocarbon molecules, are typically hydrophilic whereas the microchannels encountered in this study are hydrophobic, the acetonitrile solvent molecules being surrounded by the hydrocarbon portion of the spacer molecules. In three instances the acetonitrile molecules were observed to be disordered, possibly dynamically. We have not yet investigated in detail the influence of the solvent on cocrystal formation and whether or not the cocrystals are capable of selectively enclathrating from solvent mixtures. However, given that solvent choice can be a critical factor in whether or not superdiamondoid networks can even be crystallized[4a] this is an aspect of the chemistry which we plan to pursue.

Crystal polarity. The diamondoid architecture is more than aesthetically pleasing. A feature of tetrahedral molecules is that they do not possess an inversion centre. Hence, given that crystal packing can often be regarded as a manifestation of molecular self-assembly, one could reasonably assume that crystals based upon tetrahedral architecture are predisposed to crystallize in polar space groups since self-assembly can be controlled in three dimensions. Unfortunately, only three of the compounds studied herein adopt polar space groups, a consequence of the ability of the spacer molecule to sit or disorder around a crystallographic inversion centre. Nevertheless, rational design of polar crystals remains an important consideration in crystal engineering since piezoelectric, ferroelectric and second-order non-linear optical effects are exhibited by polar crystals.[43] Furthermore, one of the more important non-linear optic and ferroelectric materials is KH_2PO_4, a compound which has a tertiary crystal structure that is not based exclusively upon ionic packing. The tertiary crystal structure is the consequence of self-assembly of $H_2PO_4^-$ anions into a diamondoid network. Potassium cations interact with oxygen atoms in such a manner that what can be regarded as a second diamondoid framework exists.[44]

In summary, the nature of diamondoid networks formed between $[\{M(CO)_3(\mu_3\text{-}OH)\}_4]$ (M = Mn or Re) and difunctional hydrogen-bond-acceptor spacer molecules is profoundly and predictably influenced by the spacer. It is clear that suitable difunctional hydrogen-bond acceptors, even arenes, can sustain three-dimensional diamondoid networks which can have physical features similar to zeolites even though their chemical nature is markedly different. Generation of networks with low degrees of interpenetration appears to be an attainable[4] and desirable goal, especially one-fold networks that could in principle have up to 50% of their volume as space for enclathration of guest molecules.

Experimental

Synthetic Procedures.—1,2-Diaminoethane, 4,4'-bipyridyl, 1,2-diaminobenzene, *N,N,N',N'*-tetramethylethane-1,2-diamine, 4,4'-bipiperidine and 2-chloropyrazine and all solvents including toluene and *p*-xylene (Aldrich) and $[Mn_2(CO)_{10}]$ and $[Re_2(CO)_{10}]$ (Strem Chemical Co.) were used as received. All solvents were distilled over calcium hydride and stored over molecular sieves prior to use. The compound $[\{Re(CO)_3(\mu_3\text{-}OH)\}_4]$ **2** was prepared as described in the literature[10] and $[\{Mn(CO)_3(\mu_3\text{-}OH)\}_4]$ **1** was prepared as described by Clerk and Zaworotko.[8b]

Infrared spectra were recorded on a Perkin-Elmer FT 1600 series instrument. The solid-state ^1H NMR spectrum of **1**·2bipy·2MeCN was recorded on a Nicolet 360-NB instrument at the Atlantic Regional Magnetic Resonance Centre, Halifax, Nova Scotia, Canada and microanalysis results were obtained from Canadian Microanalytical Services Ltd., Delta, B.C., Canada.

Crystals of the superdiamondoid networks were grown as follows.

$[\{Mn(CO)_3(\mu_3\text{-}OH)\}_4]\cdot 2C_6H_5Me$, **1**·$2C_6H_5Me$. Crude product (10.0 g) from the reaction of $[Mn_2(CO)_{10}]$ (12.4 g, 31.9 mmol) and $Me_3NO\cdot 2H_2O$[9b] (21.3 g, 191 mmol) was digested in boiling toluene and filtered while hot to remove insoluble material (*e.g.* $Me_3NO\cdot 2H_2O$, trimethylammonium carbonate). The resulting dark orange solution was cooled at 5 °C to form large crystals of **1**·$2C_6H_5Me$ (9.54 g, 11.8 mmol, 74% yield). A second crop (3.11 g, 3.85 mmol, 24%) was obtained after concentrating the mother-liquor. M.p., decomposes above 100 °C. IR (KBr reflectance, cm^{-1}): ν_{OH} 3566; ν_{CO} 2027, 1926; 838, 753 and 684 (toluene) (Found: C, 38.65; H, 2.30. Calc. for $C_{26}H_{20}Mn_4O_{16}$: C, 38.40; H, 2.50%).

$[\{Mn(CO)_3(\mu_3\text{-}OH)\}_4]\cdot 2C_6H_6$, **1**·$2C_6H_6$. The compound **1**·$2C_6H_5Me$ (0.50 g, 0.62 mmol) was dissolved in acetonitrile (20 cm^3) at room temperature. Benzene (12 cm^3) was added dropwise until precipitation occurred. The slurry was then heated to boiling (clear solution) and allowed to cool slowly, affording crystals of **1**·$2C_6H_6$, decomposes above 110 °C. IR (KBr reflectance, cm^{-1}): ν_{OH} 3573; ν_{CO} 2028, 1938, 1887, 1871 and 1852.

$[\{Mn(CO)_3(\mu_3\text{-}OH)\}_4]\cdot 2C_6H_4Me_2\text{-}1,4$, **1**·$2C_6H_4Me_2\text{-}1,4$. The compound **1**·$2C_6H_5Me$ (0.25 g, 0.31 mmol) was dissolved in hot *p*-xylene (30 cm^3) and allowed to cool to room temperature. Yellow microcrystals of the product were formed (0.14 g, 0.17 mmol, 55% yield), decomposes above 140 °C. IR (KBr reflectance, cm^{-1}): ν_{OH} 3566; ν_{CO} 2029, 1937; 841, 814 and 684 (*p*-xylene). These crystals were too small for X-ray crystallography. Suitable single crystals were obtained from a solution containing butyric acid, a crystallization aid used in an earlier study of diamondoid networks.[6a]

$[\{Mn(CO)_3(\mu_3\text{-}OH)\}_4]\cdot 2MeC_6H_4F\text{-}4$, **1**·$2MeC_6H_4F\text{-}4$. A supersaturated solution was prepared by adding the compound **1**·$2C_6H_5Me$ (0.40 g, 0.50 mmol) to hot *p*-fluorotoluene (20 cm^3). The solution was filtered and allowed to cool slowly to room temperature affording crystals of **1**·$2MeC_6H_4F\text{-}4$, decomposes above 120 °C. IR (KBr reflectance, cm^{-1}): ν_{OH} 3578; ν_{CO} 2032, 1931 and 1892.

$[\{Mn(CO)_3(\mu_3\text{-}OH)\}_4]\cdot 2C_{10}H_8$, **1**·$2C_{10}H_8$. A saturated room-temperature solution (20 cm^3) of naphthalene in methylcyclohexane–chloroform (2:1) was prepared. The compound **1**·$2C_6H_5Me$ was added (0.50 g, 0.62 mmol). The solution was heated to boiling and acetonitrile (4 cm^3) was added completely to dissolve the **1**·$2C_6H_5Me$. The solution was cooled slowly to room temperature to afford crystals of **1**·$2C_{10}H_8$, decomposes above 115 °C. IR (KBr reflectance, cm^{-1}): ν_{OH} 3572; ν_{CO} 2028, 1938, 1906 and 1886.

$[\{Mn(CO)_3(\mu_3\text{-}OH)\}_4]\cdot 2C_{10}H_7Me\text{-}1$, **1**·$2C_{10}H_7Me\text{-}1$. The compound **1**·$2C_6H_5Me$ (0.60 g, 0.74 mmol) was added to 1-methylnaphthalene (15 cm^3). The solution was heated until clear, filtered whilst hot and allowed to cool slowly to room temperature, affording crystals of the desired product, decomposes above 110 °C. IR (KBr reflectance, cm^{-1}): ν_{OH} 3556; ν_{CO} 2029, 1938 and 1887.

$[\{Mn(CO)_3(\mu_3\text{-}OH)\}_4]\cdot$2tmen, **1**·2tmen. The compound **1**·$2C_6H_5Me$ (0.50 g, 0.62 mmol) was dissolved in MeCN (5 cm^3) and to this clear solution was added *N,N,N',N'*-tetramethylethane-1,2-diamine (0.143 g, 1.24 mmol) in MeCN (5 cm^3). The resulting solution was allowed to stand at room temperature and deposited well developed crystals of **1**·2tmen (0.30 g, 0.35 mmol, 56% yield), gradually decomposes above 160 °C. IR (KBr reflectance, cm^{-1}): $\nu_{OH,NH}$ 3122 (br with shoulders); ν_{CH} 2964, 2853, 2788; ν_{CO} 2102, 2010 and 1912.

$[\{Mn(CO)_3(\mu_3\text{-}OH)\}_4]\cdot$2dppoe·MeCN, **1**·2dppoe·MeCN. 1,2-bis(diphenylphosphoryl)ethane (0.53 g, 1.2 mmol) was dissolved in boiling MeCN (15–20 cm^3) to which a solution of **1**·$2C_6H_5Me$ (0.50 g, 0.62 mmol) dissolved in MeCN (5 cm^3) was added. The mixture formed fine pale yellow crystals of the adduct upon standing (0.87 g, 0.57 mmol, 92% yield). The product was recrystallized from boiling MeCN (35–40 cm^3) to afford large single crystals suitable for X-ray diffraction, decomposes above 135 °C. IR (KBr reflectance, cm^{-1}): ν_{OH} 3196; ν_{CO} 2015 and 1910.

$[\{Re(CO)_3(\mu_3\text{-}OH)\}_4]\cdot$2dab·4MeCN, **2**·2dab·4MeCN. Compound **2** (0.057 g, 0.049 mmol) was dissolved in MeCN (3 cm^3) and a solution of 1,4-diaminobenzene (0.011 g, 0.10 mmol) in MeCN (3 cm^3) was added. The microcrystalline precipitate (0.073 g, 0.048 mmol, 98% yield) that formed immediately was filtered off, dried, redissolved in boiling MeCN (20 cm^3) and allowed to cool slowly. Large crystals of **2**·2dab·4MeCN (0.060 g, 0.040 mmol, 80% yield) were formed. The colour changed slowly from colourless to brown above 230 °C and to black above 260 °C. Did not melt up to 300 °C. IR (KBr reflectance, cm^{-1}): ν_{OH} 3318; ν_{CH} 3276, 3160; ν_{NH} 2864; ν_{CO} 2021, 1905 and 1870.

$[\{Mn(CO)_3(\mu_3\text{-}OH)\}_4]\cdot$2en, **1**·2en. The compound **1**·$2C_6H_5Me$ (0.50 g, 0.62 mmol) was dissolved in dry freshly distilled toluene (30 cm^3) and gently warmed. This solution was stirred and en (0.074 g, 1.2 mmol) was added dropwise. A yellow precipitate formed instantaneously and the toluene solution became colourless. The reaction mixture was cooled in an ice-bath and filtered. The resulting yellow product (0.36 g, 0.50 mmol, 80% yield) was recrystallized from hot MeCN (30 cm^3) to afford yellow-brown crystals. A second batch was obtained by cooling the mother-liquor at 5 °C. IR (KBr reflectance, cm^{-1}): $\nu_{OH,NH}$ 3375; ν_{CO} 2011 and 1916 (Found: C, 25.85; H, 2.70; N, 7.55. Calc. for $C_{16}H_{20}Mn_4N_4O_{16}$: C, 26.10; H, 2.70; N, 7.25%).

$[\{Mn(CO)_3(\mu_3\text{-}OH)\}_4]\cdot$2cpyz, **1**·2cpyz. The compound **1**·$2C_6H_5Me$ (0.50 g, 0.62 mmol) and 2-chloropyrazine (0.142 g, 1.24 mmol) were each dissolved in MeCN (5 cm^3) and then mixed. The resulting solution was diluted with chloroform (10 cm^3), layered with hexanes and cooled in a freezer at −15 °C for several days. Dark yellow crystals of **1**·2cpyz (0.32 g, 0.37 mmol, 60% yield) were obtained, decomposes above 135 °C. IR (KBr reflectance, cm^{-1}): ν_{OH} 3593; ν_{CO} 2026 and 1929.

$[\{Mn(CO)_3(\mu_3\text{-}OH)\}_4]\cdot$2bipy·2MeCN, **1**·2bipy·2MeCN. The compound **1**·$2C_6H_5Me$ (0.50 g, 0.62 mmol) was dissolved in dry freshly distilled toluene (30 cm^3) and MeCN (25 cm^3) by gentle warming. A clear solution of 4,4'-bipyridyl (0.190 g, 1.23 mmol) in MeCN (25 cm^3) was added dropwise and a yellow solid (0.40 g, 0.39 mmol, 63%) precipitated immediately. It was dissolved in MeCN and stored at 5 °C for 7 d, at which point single crystals (0.38 g, 0.37 mmol) of **1**·2bipy·2MeCN were afforded, decomposes above 130 °C. IR (KBr reflectance, cm^{-1}): $\nu_{OH,NH}$ 3375; ν_{CH} 2941; ν_{CO} 2018 and 1909.

$[\{Re(CO)_3(\mu_3\text{-}OH)\}_4]\cdot$2bipy·2MeCN, **2**·2bipy·2MeCN. Compound **2** (0.0768 g, 0.0668 mmol) was dissolved in MeCN (1 cm^3) and a solution of 4,4'-bipyridyl (0.0107 g, 0.0685 mmol) in MeCN (1 cm^3) was added. A white crystalline powder (0.087 g, 0.056 mmol, 61% yield) formed immediately, was filtered off and dried. It was dissolved in boiling MeCN (5 cm^3) and allowed to stand at room temperature for crystallization.

Table 3 Summary of data collection and structure refinement parameters

	1·2C$_6$H$_6$	1·2C$_6$H$_5$Me	1·2C$_6$H$_4$Me$_2$-1,4	1·2MeC$_6$H$_4$F-4	1·2C$_{10}$H$_8$	1·2C$_{10}$H$_7$Me-1	1·2tmen
Formula (excluding solvent)	$C_{24}H_{16}Mn_4O_{16}$	$C_{26}H_{20}Mn_4O_{16}$	$C_{28}H_{24}Mn_4O_{16}$	$C_{26}H_{18}F_2Mn_4O_{16}$	$C_{32}H_{20}Mn_4O_{16}$	$C_{34}H_{24}Mn_4O_{16}$	$C_{24}H_{36}Mn_4O_{16}$
M	780.13	808.2	836.2	844.17	880.24	908.31	856.3
Crystal dimensions/mm	0.35 × 0.40 × 0.40	0.40 × 0.60 × 0.80	0.10 × 0.20 × 0.20	0.30 × 0.30 × 0.40	0.20 × 0.30 × 0.40	0.30 × 0.50 × 0.70	0.70 × 0.80 × 0.90
Crystal colour	Orange-brown	Orange	Orange	Orange	Brown	Brown	Orange
Crystal system	Cubic	Tetragonal	Tetragonal	Tetragonal	Tetragonal	Hexagonal	Tetragonal
Space group	$Pn\bar{3}m$	$P4_2/nnm$	$P4_2/nnm$	$P4_2/nnm$	$I4_1/acd$	$R\bar{3}$	$P4_122$ or $P4_322$
a/Å	11.2472(4)	11.1206(8)	11.0282(6)	11.0312(10)	17.5574(12)	35.020(10)	10.8233(6)
c/Å	—	12.6696(15)	13.6219(12)	12.9418(18)	22.333(3)	20.513(4)	32.652(3)
U/Å^3	1422.77(5)	1566.82(22)	1656.71(17)	1574.9(3)	6884.6(10)	21787(8)	3824.9(4)
Z	2	2	2	2	8	24	4
D_c/g cm^{-3}	1.82	1.71	1.68	1.78	1.70	1.66	1.49
F(000)	776	808	840	840	3520	10 944	1744
μ/cm^{-1}	17.4	15.8	15.0	15.9	14.5	13.8	13
Transmission range	0.71–1.00	0.64–1.00	0.78–1.00	0.74–1.00	0.71–1.00	0.64–1.00	0.72–1.00
$2\theta_{max}$/°	49.8	49.8	50	44.9	44.8	40	45
Data collected	1249	1382	795	1037	1981	7167	4972
Independent data	264	748	795	567	1023	4515	2499
Observed data [$I_{obs} \geq 3\sigma(I)$]	213	514	446	426	648	2814	2093
Parameters refined	28	64	67	64	118	667	218
R	0.042	0.032	0.031	0.042	0.030	0.046	0.037
R'	0.052	0.036	0.030	0.049	0.028	0.037	0.05
Goodness of fit[a]	5.09	3.11	1.87	5.88	1.82	2.91	3.99
Final shift/error residual	0.001	0.000	0.000	0.000	0.000	0.010	0.003

	1·2dppoe	2·2dab	1·2en	1·2cpyz	1·2bipy	2·2bipy	1·2bipip
Formula (excluding solvent)	$C_{64}H_{52}Mn_4O_{20}P_4$	$C_{24}H_{20}N_4O_{16}Re_4$	$C_{16}H_{20}Mn_4N_4O_{16}$	$C_{20}H_{10}Cl_2Mn_4N_4O_{16}$	$C_{32}H_{20}Mn_4N_4O_{16}$	$C_{32}H_{20}N_4O_{16}Re_4$	$C_{32}H_{44}Mn_4N_4O_{16}$
M	1484.7	1365.3	744.1	853	936.3	1461.4	960.5
Crystal dimensions/mm	0.30 × 0.40 × 0.50	0.20 × 0.40 × 0.80	0.25 × 0.30 × 0.50	0.20 × 0.30 × 0.40	0.20 × 0.20 × 0.40	0.20 × 0.20 × 0.40	0.20 × 0.20 × 0.50
Crystal colour	Orange	Colourless	Orange	Orange	Orange	Colourless	Yellow
Solvent molecules	MeCN	4MeCN	—	—	2MeCN	2MeCN	2MeCN
Crystal system	Tetragonal	Tetragonal	Cubic	Cubic	Tetragonal	Tetragonal	Tetragonal
Space group	$P4_2/n$	$P4_2/n$	$I\bar{4}3d$	$I\bar{4}3d$	$P4/nnc$	$P4/nnc$	$P4/n$
a/Å	14.2907(14)	15.1361(22)	20.733(3)	21.1501(16)	13.984(4)	14.1370(17)	14.7355(13)
c/Å	18.001(3)	9.9037(21)	—	—	23.416(9)	22.938(4)	11.2727(14)
U/Å^3	3676.2(8)	2269.0(6)	8912.2(13)	9461.0(12)	4579.1(22)	4584.3(10)	2447.7(4)
Z	2	2	12	12	4	4	2
D_c/g cm^{-3}	1.38	2.24	1.66	1.79	1.48	2.24	1.41
F(000)	1556	1416	4480	5040	2048	2848	1072
μ/cm^{-1}	7.9	108.4	22.1	16.6	11	107	10
Transmission range	[b]	0.21–0.77	[b]	[b]	[b]	0.57–0.99	0.91–1.00
$2\theta_{max}$/°	45	49.9	45	45	40	45	45
Data collected	2641	2151	1725	946	2006	1517	1747
Independent data	2408	1991	523	568	1087	1507	1605
Observed data [$I_{obs} \geq 3\sigma(I)$]	1279	1281	458	397	665	876	854
Parameters refined	206	136	95	109	141	94	139
R	0.063	0.051	0.027	0.040	0.040	0.073	0.043
R'	0.063	0.059	0.026	0.035	0.048	0.082	0.043
Goodness of fit[a]	3.15	3.45	1.90	2.47	2.79	4.34	2.29
Final shift/error residual	0.000	0.000	0.001	0.009	0.000	0.000	0.003

[a] $[w(|F_o| - |F_c|)^2/(N_{observations} - N_{variables})]^{\frac{1}{2}}$. [b] No correction was made for absorption.

Crystals (0.07 g) were obtained after 7 d. They changed slowly from white to brown above 180 °C and to dark above 280 °C, m.p. > 300 °C. IR (KBr reflectance, cm^{-1}): ν_{OH} 3350; ν_{CH} 3276, 3160; ν_{CO} 2024, 1905 and 1880.

[{Mn(CO)$_3$(μ_3-OH)}$_4$]·2bipip·2MeCN, **1**·2bipip·2MeCN. The compound **1**·2C$_6$H$_5$Me (0.25 g, 0.31 mmol) and 4,4′-bipiperidine (0.104 g, 0.618 mmol) were each dissolved in MeCN (30 cm^3). The two solutions were mixed and a bright yellow precipitate (0.24 g, 0.22 mmol, 70%) formed immediately. It was redissolved in hot MeCN (50 cm^3) and cooled to room temperature. Yellow single crystals formed upon standing. A second crop was obtained by cooling the initial filtrate to 5 °C, decomposes above 130 °C. IR (KBr reflectance, cm^{-1}): $\nu_{OH,NH}$ 3415; ν_{CH} 2911; ν_{CO} 2020 and 1911.

X-Ray Crystallography.—Single crystals were mounted in thin-walled glass capillaries and placed on an Enraf-Nonius CAD-4 diffractometer. Unit-cell dimensions were determined *via* least-squares refinement of the setting angles of 24 high-angle reflections and intensity data were collected using the ω–2θ scan mode. Data were corrected for Lorentz, polarization and absorption (where directed by crystal shape or absorption coefficient) effects but not for extinction. In several compounds, poor scattering, which we attribute to disorder and/or high thermal motion in solvent or spacer molecules, precluded collection of data to a 2θ limit of 50°. However, this in no way prejudices our assignment of space group or interpretation of the crystal packing.

1·2C$_6$H$_5$Me. Pertinent data collection and structure refinement parameters are presented in Table 3. The structure was solved using direct methods and all non-hydrogen atoms were refined with anisotropic thermal parameters. Compound **1** was found to lie around crystallographic $\bar{4}2m$ positions whereas the toluene spacer molecules lay around $2/m$ positions. The toluene methyl groups are therefore disordered between two sites and were refined with an occupancy factor of 0.50. Hydrogen atoms were located *via* Fourier-difference map inspection (OH, CH) or calculated (CH: sp^2, D_{C-H} = 1.00 Å; sp^3, D_{C-H} = 1.08 Å), given isotropic thermal parameters based upon the atom to which they are bonded, and fixed during least-squares refinement. Weights based upon counting statistics were used with the weight modifier, k, in $kF_o{}^2$ being determined *via* evaluation of the variation in standard reflections during the course of data collection. Values of R and R' were given by $\Sigma(|F_o| - |F_c|)/\Sigma|F_o|$ and $[\Sigma w(|F_o| - |F_c|)^2/\Sigma(wF_o{}^2)]^{\frac{1}{2}}$. All crystallographic calculations were effected using the PC version of the NRCVAX suite of programs[45] and 80486-based IBM-compatible computers. Scattering factors were taken from ref. 46. Crystallographic figures were drawn using ORTEP[30] or PLUTO.[47]

1·2C$_6$H$_6$. As above except as follows. Molecules of compound **1** lie around crystallographic $\bar{4}3m$ positions; molecules of benzene are located around $\bar{3}m$ positions; there is no disorder; all hydrogen atoms were located *via* Fourier-difference map inspection and refined.

1·2C$_6$H$_4$Me$_2$-1,4. As before but no disorder of the methyl groups.

1·2MeC$_6$H$_4$F-4. As before except the disorder is between the methyl group and the fluorine atom; the disordered carbon and fluorine atoms were refined as an oxygen atom with a site occupancy factor of $\frac{15}{16}$.

1·2C$_{10}$H$_8$. As before except as follows: molecules of compound **1** are located around $\bar{4}$ positions; naphthalene molecules reside around $\bar{1}$ positions; there is no disorder.

1·2C$_{10}$H$_7$Me-1. As before except as follows: two independent molecules of compound **1** are located around three-fold axes and general positions, respectively; there are four independent molecules of 1-methylnaphthalene, two located at general positions, one disordered around a $\bar{1}$ position, and one disordered around a $\bar{3}$ position; sp^3 hydrogen atoms were calculated and fixed with D_{C-H} = 1.08 Å.

1·2tmen. As before except as follows: the only crystallographically imposed symmetry arises from compound **1** lying around two-fold axes; CH$_2$ hydrogen atoms were placed in calculated positions (D_{C-H} = 1.08 Å); it was not possible to distinguish between the space group $P4_122$ and its enantiomorph $P4_322$ despite collection and refinement of Friedel equivalent reflections (Rogers[48] η = 0.00).

1·2dppoe. As before except as follows: molecules of compound **1** are located around crystallographic $\bar{4}$ positions; the spacer molecules were disposed around inversion centres with the phenyl and ethylene moieties 50% disordered; a disordered MeCN molecule was located at a crystallographic $\bar{4}$ position and refined with fixed isotropic thermal parameters and variable site occupancy factors.

2·2dab. As for **1**·2dppoe except as follows: the solvent and spacer molecules are ordered; the solvent molecule lies in a general position and there are therefore four molecules of MeCN per molecule of **2**.

1·2en. As for **1**·2C$_6$H$_5$Me except as follows: molecules of compound **1** are located around $\bar{4}$ positions; spacer molecules are located around a two-fold axis; the OH hydrogen atom was refined.

1·2cpyz. As for **1**·2en except as follows: the spacer molecule was disordered; chlorine atoms were refined with a site occupancy factor of 0.50 whereas disorder within the pyrazine ring, manifested by high thermal motion and geometric inconsistencies, was not resolvable.

1·2bipy. As for **1**·2C$_6$H$_5$Me except as follows: the spacer molecules reside around $\bar{1}$ positions; molecules of compound **1** are located around $\bar{4}$ positions; the independent OH hydrogen atom was refined with a fixed thermal parameter; two independent disordered MeCN solvent molecules were located on crystallographic four-fold axes. Molecule A lies on a four-fold axis whereas only the central atom of molecule B resides on a four-fold axis. The outer atoms of molecule B were refined as carbon atoms with fixed thermal parameters and gave a site occupancy factor of 0.47. Solvent hydrogen atoms were not accounted for during refinement.

2·2bipy. As for **1**·2bipy except as follows: carbonyl carbon atoms were refined with isotropic thermal parameters only; quite large (> 3 e Å^{-3}) peaks were observed near Re in the final Fourier-difference map, indicative of absorption effects; the disordered solvent atoms were refined anisotropically as carbon atoms.

1·2bipip. As for **1**·2bipy except as follows: bipip molecules sit around crystallographic inversion centres; the two independent MeCN solvent molecules lie on crystallographic two-fold axes and were refined isotropically.

Additional material available from the Cambridge Crystallographic Data Centre comprises all atomic coordinates, thermal parameters and remaining bond lengths and angles.

Acknowledgements

We thank the National Sciences and Engineering Research Council, Canada (research grant to M. J. Z.; undergraduate research award to J. O. S. S.), The Institute for Chemical Science and Technology, Canada and Saint Mary's University (Senate Research Grants, purchase of the X-ray diffractometer) for financial support of this work. The NMR spectra were recorded at the Atlantic Region Magnetic Resonance Centre by Dr. Donald Hooper.

References

1 See, for example, (*a*) C. V. Krishnamohan, K. Panneerselvam, T. Pilati and G. R. Desiraju, *J. Chem. Soc., Chem. Commun.*, 1992, 832; (*b*) F. Garcia-Tallado, S. J. Geib, S. Goswami and A. D. Hamilton, *J. Am. Chem. Soc.*, 1991, **113**, 9265; (*c*) S. J. Geib, S. C. Hirst, C. Vicent and A. D. Hamilton, *J. Chem. Soc., Chem. Commun.*, 1991, 1283; (*d*) X. Zhao, Y.-L. Chang, F. W. Fowler and

J. W. Lauher, *J. Am. Chem. Soc.*, 1990, **112**, 6627; (*e*) J.-M. Lehn, M. Mascal, A. DeCian and J. Fischer, *J. Chem. Soc., Chem. Commun.*, 1990, 479; (*f*) M. C. Etter, *Acc. Chem. Res.*, 1990, **23**, 120; (*g*) C. B. Aakeroy, P. B. Hitchcock and K. R. Seddon, *J. Chem. Soc., Chem. Commun.*, 1992, 553; (*h*) G. R. Desiraju, in *Crystal Engineering. The Design of Organic Solids*, Elsevier, Amsterdam, 1989; (*i*) J. A. Zerkowski and G. M. Whitesides, *J. Am. Chem. Soc.*, 1994, **116**, 4298; (*j*) J. A. Zerkowski, J. P. Mathias and G. M. Whitesides, *J. Am. Chem. Soc.*, 1994, **116**, 4305; (*k*) Y.-L. Chang, M.-A. West, F. W. Fowler and J. W. Lauher, *J. Am. Chem. Soc.*, 1993, **115**, 5991; (*l*) S. Hanessian, A. Gomtsyan, M. Simard and S. Roelens, *J. Am. Chem. Soc.*, 1994, **116**, 4495; (*m*) V. A. Russell, M. C. Etter and M. D. Ward, *J. Am. Chem. Soc.*, 1994, **116**, 1941; (*n*) A. T. Ung, R. Bishop, D. C. Craig, I. G. Dance and M. L. Scudder, *J. Chem. Soc., Chem. Commun.*, 1993, 322; (*o*) C. B. Aakeroy and M. Nieuwenhuyzen, *J. Am. Chem. Soc.*, 1994, **116**, 10983.

2 L. Pauling, *The Nature of The Chemical Bond*, 2nd edn., Cornell University Press, Ithaca, New York, 1948.

3 (*a*) O. Ermer, *J. Am. Chem. Soc.*, 1988, **110**, 3747; (*b*) O. Ermer and A. Eling, *Angew. Chem., Int. Ed. Engl.*, 1988, **27**, 829.

4 (*a*) M. Simard, D. Su and J. D. Wuest, *J. Am. Chem. Soc.*, 1991, **113**, 4696; (*b*) O. Ermer and L. Lindenberg, *Helv. Chim. Acta*, 1991, **74**, 825; (*c*) O. Ermer and L. Lindenberg, *Chem. Ber.*, 1990, **123**, 1111; (*d*) O. Ermer and L. Lindenberg, *Helv. Chim. Acta*, 1988, **71**, 1084.

5 S. B. Copp, S. Subramanian and M. J. Zaworotko, *J. Am. Chem. Soc.*, 1992, **114**, 8719; *J. Chem. Soc., Chem. Commun.*, 1993, 1078; M. J. Zaworotko, *Chem. Soc. Rev.*, 1994, 283.

6 J. S. Lindsey, *New J. Chem.*, 1991, **15**, 153.

7 D. S. Reddy, D. C. Craig, A. D. Rae and G. R. Desiraju, *J. Chem. Soc., Chem. Commun.*, 1993, 1737.

8 (*a*) M. Herberhold, F. Wehrmann, D. Neugebauer and G. Huttner, *J. Organomet. Chem.*, 1978, **152**, 329; (*b*) M. D. Clerk and M. J. Zaworotko, *J. Chem. Soc., Chem. Commun.*, 1991, 1607.

9 M. D. Clerk, S. B. Copp, S. Subramanian and M. J. Zaworotko, *Supramolecular Chem.*, 1992, **1**, 7.

10 M. Herberhold and G. Suss, *Angew. Chem., Int. Ed. Engl.*, 1975, **87**, 750.

11 (*a*) E. Horn, M. R. Snow and P. C. Zeleny, *Aust. J. Chem.*, 1980, **33**, 1659; (*b*) B. Nuber, F. Oberdorfer and M. L. Ziegler, *Acta Crystallogr., Sect. B*, 1981, **37**, 2062.

12 P. A. Aubry, J. Protas, E. Moreno-Gonzalez and M. Marraud, *Acta Crystallogr., Sect. B*, 1977, **33**, 2572.

13 J. L. Atwood, F. Hamada, K. D. Robinson, G. W. Orr and R. L. Vincent, *Nature (London)*, 1991, **349**, 683.

14 H. S. Szepa, M. L. Webb, A. M. Z. Slawin and D. J. Williams, *J. Chem. Soc., Chem. Commun.*, 1991, 765.

15 A. D. U. Hardy and D. D. MacNicol, *J. Chem. Soc., Perkin Trans. 2*, 1976, 1140.

16 K. Nakatsu, H. Yoshioka and K. Kunimoto, *Acta Crystallogr., Sect. B*, 1978, **34**, 2357.

17 S. S. Al-Juaid, A. K. A. Al-Nasr, C. Eaborn and P. B. Hitchcock, *J. Chem. Soc., Chem. Commun.*, 1991, 1482.

18 L. R. Hanton, C. A. Hunter and D. H. Purvis, *J. Chem. Soc., Chem. Commun.*, 1992, 1134.

19 M. Oki and H. Iwamura, *J. Am. Chem. Soc.*, 1967, **89**, 576; M. R. Basila, E. L. Saier and L. R. Cousins, *J. Am. Chem. Soc.*, 1965, **87**, 1665; S. Suzuki, P. G. Green, R. E. Bumgarner, S. Dasgupta, W. A. Goddard III and G. A. Blake, *Science*, 1992, **257**, 942.

20 M. A. Viswamitra, R. Radhakrishnan, J. Bandekar and G. R. Desiraju, *J. Am. Chem. Soc.*, 1993, **115**, 4868.

21 W. L. Jorgenesen and D. L. Severance, *J. Am. Chem. Soc.*, 1990, **112**, 4768; B. V. Cheney, M. W. Schulz and W. G. Richards, *J. Am. Chem. Soc.*, 1988, **110**, 4195.

22 P. D. Bakshi, A. Linden, B. R. Vincent, S. P. Roe, D. Adhikesavalu, T. S. Cameron and O. Knop, *Can. J. Chem.*, 1993, **72**, 1273.

23 J. E. Cochran, T. J. Parrott, B. J. Whitlock and H. W. Whitlock, *J. Am. Chem. Soc.*, 1992, **114**, 2269.

24 J. L. Atwood, S. G. Bott, C. Jones and C. L. Raston, *J. Chem. Soc., Chem. Commun.*, 1992, 1349.

25 A. Irving and H. M. N. H. Irving, *J. Crystallogr. Spectrosc. Res.*, 1993, **23**, 725; (*b*) A. Irving, R. Hunter and R. H. Haueisen, *J. Chem. Crystallogr.*, 1994, **24**, 267.

26 M. J. Zaworotko, K. C. Sturge, L. Nunez and R. D. Rogers, *Organometallics*, 1991, **10**, 1806.

27 G. R. Desiraju, *Acc. Chem. Res.*, 1991, **24**, 290.

28 K. T. Holman and M. J. Zaworotko, *J. Chem. Crystallogr.*, in the press.

29 L. Shimoni, H. L. Carrell, J. P. Glusker and M. M. Coombs, *J. Am. Chem. Soc.*, 1994, **116**, 8162.

30 C. K. Johnson, ORTEP, A Fortran Thermal Ellipsoid Plot Program, Technical Report ORNL-5138, Oak Ridge National Laboratory, Oak Ridge, TN, 1976.

31 G. C. Pimentel and A. L. McLellan, in *The Hydrogen Bond*, W. H. Freeman, San Francisco, 1960.

32 C. E. Holloway and M. Melnik, *J. Organomet. Chem.*, 1990, **396**, 129.

33 S. B. Copp, S. Subramanian and M. J. Zaworotko, *Angew. Chem., Int. Ed. Engl.*, 1993, **32**, 706.

34 B. F. Abrahams, M. J. Hardie, B. F. Hoskins, R. Robson and G. A. Williams, *J. Am. Chem. Soc.*, 1992, **114**, 10 641 and refs therein.

35 D. Craig, I. G. Dance and R. Garbutt, *Angew. Chem., Int. Ed. Engl.*, 1986, **25**, 165.

36 K.-W. Kim and M. G. Kanatzidis, *J. Am. Chem. Soc.*, 1992, **114**, 4878.

37 R. Robson, B. F. Abrahams, S. R. Batten, R. W. Gable, B. F. Hoskins and J. Liu, *ACS Symp. Ser.*, 1992, **499**, 256; L. R. MacGillivray, S. Subramanian and M. J. Zaworotko, *J. Chem. Soc., Chem. Commun.*, 1994, 1325; K. Sinzger, S. Hunig, M. Jopp, D. Bauer, W. Bietsch, J. U. von Schutz, H. C. Wolf, R. K. Kremer, T. Metzenthin, R. Bau, S. I. Khan, A. Lindbaum, C. L. Lengauer and E. Tillmanns, *J. Am. Chem. Soc.*, 1993, **115**, 7696.

38 T. Kitazawa, S. Nishikiori, R. Kuroda and T. Iwamoto, *Chem. Lett.*, 1988, 1729.

39 S. Nishikiori, C. I. Ratcliffe and J. A. Ripmeester, *J. Am. Chem. Soc.*, 1992, **114**, 8590.

40 D. M. Proserpio, R. Hoffmann and P. Preuss, *J. Am. Chem. Soc.*, 1994, **116**, 9634.

41 O. Ermer and A. Eling, *J. Chem. Soc., Perkin Trans. 2*, 1994, 925.

42 R. M. Barrer, in *Zeolites and Clay Minerals as Sorbents and Molecular Sieves*, Academic Press, New York, 1978; L. A. Mundi and R. C. Haushalter, *Chem. Mater.*, 1992, **4**, 31.

43 *International Tables for X-Ray Crystallography*, Kluwer, Dordrecht, 1989, vol. A, pp. 786–791.

44 S. Endo, T. Chino, S. Tsuboi and K. Koto, *Nature (London)*, 1989, **340**, 452 and refs. therein.

45 E. J. Gabe, Y. Le Page, J.-P. Charland, F. L. Lee and P. S. White, *J. Appl. Crystallogr.*, 1989, **22**, 384.

46 *International Tables for X-Ray Crystallography*, Kynoch Press, Birmingham, 1974, vol. 4.

47 W. O. S. Motherwell and W. Clegg, PLUTO 78, University of Cambridge, 1978.

48 D. Rogers, *Acta Crystallogr., Sect. A*, 1981, **37**, 734.

Received 13*th January* 1995; *Paper* 5/00218D